Article ID: 1006-8775(2009) 01-0028-09

RESEARCH ON AUTOMATIC FOG IDENTIFICATION TECHNOLOGY BY METEOROLOGICAL SATELLITE REMOTE SENSING

ZHOU Hong-mei (周红妹), GE Wei-qiang (葛伟强), BAI Hua (柏桦),
LIU Dong-wei (刘冬韡), YANG Ying-min (杨引明)

(Shanghai Center for Satellite Remote-sensing and Application, Shanghai , 201100 China)

Abstract: There is an urgent need for the development of a method that can undertake rapid, effective, and accurate monitoring and identification of fog by satellite remote sensing, since heavy fog can cause enormous disasters to China's national economy and people's lives and property in the urban and coastal areas. In this paper, the correlative relationship between the reflectivity of land surface and clouds in different time phases is found, based on the analysis of the radiative and satellite-based spectral characteristics of fog. Through calculation and analyses of the relative variability of the reflectivity in the images, the threshold to identify quasi-fog areas is generated automatically. Furthermore, using the technique of quick image run-length encoding, and in combination with such practical methods as analyzing texture and shape fractures, smoothness, and template characteristics, the automatic identification of fog and fog-cloud separation using meteorological satellite remote sensing images are studied, with good results in application.

Key words: meteorological satellites remote sensing; fog; dynamic monitoring; rapid and automatic identification methods

CLC number: **Document code: A** doi: 10.3969/j.issn.1006-8775.2009.01.004

1 INTRODUCTION

Fog refers to a weather phenomenon in which visibility is reduced below 1 km. It has enormous impacts on the China's national economy and causes the most fatalities in civil aviation, water and land surface transportation, and urban highway traffic. In light of its widespread effects, research into fog monitoring started as early as the 1970s, making use of the advantages of satellite remote sensing for its rapid high resolution monitoring and wide area of coverage (Gurka et al. [1]; Gustafso et al. [2]; Gurka et al. [3]). However, most of the early analyses are case studies (Eyre et al. [4]; Turner et al. [5]; Kudoh et al. [6]; Bendix et al. [7]; Ellrod et al. [8]; Thoma et al. [9]; Bendix et al. [10]; Erasmus et al. [11]; Berthmann et al. [12]; Rosenfeld et al. [13]; Underwood et al. [14]). For instance, the Germans [15] studied fog in the Alpine and its nearby basin area, putting forth methods that concerned fog classification, image correction, and fog height determination by combining fog images with digital terrain models, and concluding with a number of useful reference indexes and calculation methods. Bendix et al.[16] used the reflection of MODIS bands 1-7 to monitor daytime fog. After calculating the reflectivity of different channels in very heavy fog (i.e., visibility of less than 50 m and thickness of 400 m) and very light fog (i.e., visibility of less than 950 m and thickness of 30 m) by using the radiation transfer equation, they used this as a threshold to determine the fog zone and separated low clouds from fog by retrieving the height of the cloud bottom. In recent years, some institutions in China have carried out research on the remote sensing of fog by using data detected with meteorological satellites [17]. For instance, in the late 1990s, in order to support the closure project for the Three Gorges dam on the Yangtze River, the National Satellite Center monitored, with some success, the coverage of heavy fog in real time with thresholds and statistical methods in conjunction with the NOAA satellite visible and infrared datasets (for daytime) and two infrared channels of data at 3.7 μm and 11 μm (for nighttime).

Received date: 2009-03-20; **revised date:** 2009-05-20
Foundation item: Key research project "Research of Shanghai City and Costal Heavy Fog Remote Sensing Detecting and Warning System" of Science and Technology Commission of Shanghai Municipality (075115011)
Biography: Zhou Hong-mei, research fellow and professor on meteorological remote sensing and GIS application research.
E-mail for correspondence author: hong_mei@163.com

Ju et al.[18] obtained preliminary achievements in monitoring the heavy fog existing on the Shanghai-Nanjing expressway using GMS-5 satellite data. Li et al.[19] carried out case studies on daytime fog using GMS-5 meteorological satellite data.

Although all of the above studies were successful to some extent, they still remain in the realm of case studies and, as such, cannot meet the operational needs of monitoring and early warning of heavy fog. This results from the usually complicated nature of cloud systems when thick fog appears, especially under conditions of the simultaneous appearance of low-lying clouds and fog. When this occurs, their spectra and brightness are very similar, and they often adhere to each other, making them difficult to distinguish. In addition, the complex manner in which the land surface reflectivity and radiation rate change, when combined with the difference in solar elevation and climate conditions that can influence the satellite-derived radiation and reflectivity, makes the separation of clouds from fog by remote sensing all the more difficult. Furthermore, due to the large volume of remote sensing image data and the complexity of the calculation procedures, there is an urgent need for the development of rapid and operationally applicable methods to identify fog automatically.

In this paper, the relative reflectivity relationships between cloud and the underlying surface, and the spectral change patterns and characteristics of underlying surfaces, cloud, and fog are recognized as being capable of automatically identifying quasi-fog areas, based on numerous analyses of remote sensing images in different time phases. Then, on the basis of the recognized quasi-fog areas and with the aid of such techniques as the analysis of spectral, textural, and structural characteristics and the rapid encoding of connected regions, the automatic identification of fog and clouds and their separation is accomplished from meteorological satellite images, meeting the need for an operational application for dynamic, rapid, and automatic fog identification.

2 PRINCIPLES OF FOG IDENTIFICATION BY REMOTE SENSING

2.1 *Radiation characteristics of fog*

Fog is composed of a large number of tiny water droplets or ice particles that exists close to the ground or floats in the air. In general, the particle radius is between a few micrometers and more than a dozen micrometers, with a density of up to several thousand cubic centimeters. When sunrays are projected upon these minute particles, light will be reflected from them in every direction. Generally known as scattering, this phenomenon is dubbed Mie scattering if it occurs in situations where the radius of atmospheric particles is equal or close to the wavelength of radiation.

Since the visible light and near-infrared wave bands are mainly sensitive to sunlight reflection and scattering radiation, when the size of the particles is equal to the visible light and near-infrared wavelength, humid weather has a large effect on the Mie scattering. This in turn will hinder and affect the satellite probe toward the land surface.

In the infrared band, the radiation characteristics of fog vary with the wavelength. Since the mid-infrared band (near 3.7 μm) is where the spectral curves of solar radiation overlap those of the earth's atmospheric radiation, the fog area not only emits radiation, but also reflects the solar radiation upward during the day; at night, it mainly radiates due to the lack of sunlight. In the long-wave infrared band (near 11 μm), fog mainly radiates upward, as its emissivity is close to 1, similar to the black body.

2.2 *Satellite spectral characteristics of fog*

According to the principles of meteorological satellite spectra, the reflectivity of vegetation, water, and soil have large differences in the band of visible light. Specifically, the surface of bare land has the highest reflectivity, followed in turn by water and vegetated surfaces. The reflectivities of clouds and fog are higher than those of water bodies, vegetated surfaces, and bare land. Compared with fog, clouds have a higher reflectivity, which varies with their shape, amount, height, and thickness. Hence, the different spectral characteristics of clouds, fog, and the underlying land surface within the visible light band make it possible to identify the cloud and fog zones.

As shown in the analysis of fog radiation characteristics in the fog zone, the albedo of fog in the near-infrared band is lower than that in the visible light band. In the visible light and near-infrared bands, the albedo of fog is higher than that of the land surface but lower than that of middle or high clouds. In the infrared band, the brightness temperature is usually lower than that of the land surface but higher than that of middle and high clouds, though it may be higher than its neighboring area when an inversion temperature layer (radiation fog) exists; the nighttime brightness temperature in the infrared band of 10.5–11.5 μm is higher than that in the 11.5–12.5 μm band and so forth.

2.3 *Structure and infrared characteristics of fog*

As shown in the visible light images from satellite remote sensing, due to the lower albedo of fog compared to those of middle, high, and thick clouds, as well as the more stable change in particle size, the structure and infrared performance of fog are

characterized by smooth and thick tops, non-transmissivity, insignificant brightness change, well-mixed texture, clear edge, closer to ambient temperatures; its texture and shape are also similar to the surrounding terrain and landforms, which are topographically identifiable. On the other hand, the cloud area has lower brightness temperature, scattered texture, irregular edge and always features shadow areas and areas of high brightness [20].

2.4 *Principles of fog automatic identification and cloud-fog separation*

In order to meet the need for automatic identification, spectral tests and analyses are conducted in this paper using multiple frames of meteorological satellite datasets for autumn and winter of recent years in the metropolitan districts of Shanghai and the coastal area, based on the characteristics of radiation and satellite spectrum principles of fog. It is found that different solar elevation angles and climate conditions will cause differences in the radiation and reflectivity of clouds, fog, and underlying surface (Fig.1) in the visible band. Besides different radiation intensities under different solar elevation angles in the areas of cloud and fog, their reflectivity is also influenced by their thickness, altitude, and climate conditions. In other words, cloud/fog areas at higher altitudes, with larger thicknesses, and stronger radiation, will have higher reflectivities. Moreover, reflectivity varies with the season and conditions of the sky. Reflectivity is much higher in spring and summer than in autumn and winter, and is also higher when the sky is clear, rather than cloudy. The reflectivity of a fog area is lower than that of a cloud area but higher than that of a land surface [21].

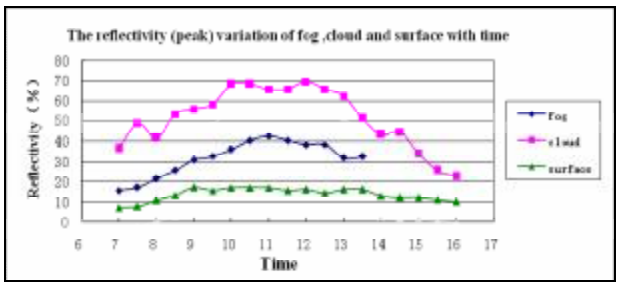

Fig.1 Reflectivity (peak) variation with time with FY－2C data. (7:00 – 16:00 L.T.)

As the difference in solar elevation and climate conditions may affect the radiation and reflectivity levels in the visible light channel, and there exists difference in the reflectivity characteristics between each frame of the visible light images of cloud, fog and underlying surface, uncertainties are caused in the discriminating thresholds for fog areas. Based on the cloud/fog reflectivity characteristics obtained for the visible light band and comprehensive study and repeated experiments on the multiple frames of remote sensing data for autumn and winter, two seasons with frequent fog formation in Shanghai and coastal areas off the East China Sea, reflectivity is found to increase with time in the morning, reach the maximum around midday (11:30), and then decrease with time (Fig.2).

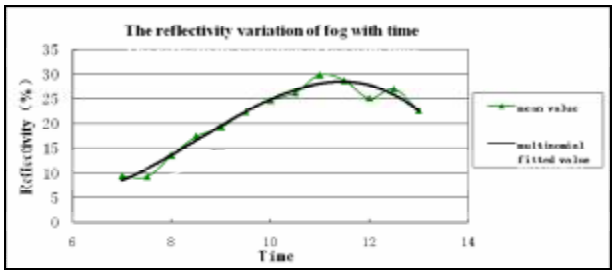

Fig.2 Mean reflectivity variation of fog with time with FY－2C data. (7:00 – 14:00 L.T.)

In addition, the experiment shows that, due to the difference in the heterogeneous scattering effect of the cloud/fog reflectivity varying with different area, height, and thickness, the land surface reflectivity may be influenced differently. When the land surface is affected by the scattering effect of high clouds, cold clouds, or the tops of convective clouds, its reflectivity will be enhanced; its magnitude is closely related to the intensity of the reflectivity of the cloud/fog.

Through the application of the aforementioned data and methods, the determination of fog areas can now be achieved more accurately, and related calculations can be executed more efficiently.

3 AUTOMATIC, RAPID DETECTION METHOD OF REMOTE SENSING OF FOG

3.1 *Satellite data selection*

To meet the needs related to the temporal resolution of dynamic fog monitoring, the FY-2C (with the ground resolution of the visible light band at 1.25 km and that of the infrared band at 5 km) and Japanese MTSAT geostationary satellites (at 1 km and 4 km respectively) are used as the main source, supplemented by data from the earth observational satellite EOS/MODIS (at 250 m and 1 km respectively). Combining ground observations with the spectral and radiative characteristics of the fog, a method of fast fog detection based on remote sensing is studied and developed to dynamically probe and extract for information from remote sensing image data.

3.2 *Fog remote sensing detection method*

3.2.1 AUTOMATIC GENERATION OF THE DYNAMIC DETERMINATION THRESHOLD OF QUASI-FOG ZONE

In this paper, due to various spectral characteristics

of the land surface and the cloud and fog zones, the reflectivity of remote sensing images is tracked and calculated for different times, and corresponding relationships are isolated between the reflectivities of the land surface medium and cloud area. Then, a dynamic quasi-fog zone discriminating threshold is automatically generated according to the calculated relative change rates for land surface media reflectivity, cloud area reflectivity, and fog reflectivity. The initial separation of fog from land surface media, middle, and high clouds is realized, and large numbers of pixels outside of the fog zone are shielded to raise the efficiency of the calculation and accuracy of identification of the algorithm that follows. The dynamic change threshold for the fog zone reflectivity determined with the FY-2C satellite is expressed as:

$$F_1(t,x,y) = h(t) + w(t) + p(x,y) \quad (1)$$

and

$$F_2(t,x,y) = h(t) - w(t) + p(x,y) \quad (2)$$

where

$$h(t) = -0.239t^3 + 6.137t^2 - 46.50t + 115.3 \quad (3)$$

$$w(t) = -0.427t^2 + 9.315t - 38.48 \quad (4)$$

$F_1(t,x,y)$ is the upper threshold of the quasi-fog zone determination threshold varying with time, *t*; $F_2(t,x,y)$ is the lower threshold of the quasi-fog zone determination threshold varying with time *t*; $h(t)$ is the mean function of the fog zone reflectivity varying with time, *t*; $w(t)$ represents the function of relative fluctuation range with time, *t*; *t* is the existence duration of the fog zone; $p(x,y)$ is the influence parameter of the land surface reflectivity affected by the cloud zone; *x* is the minimum reflectivity variable for the land surface; and *y* is the maximum reflectivity variable for the cloud zone. $p(x,y)$ is a parameter that can be calculated from a great deal of remote sensing data.

A dynamic identification threshold for quasi-fog zones is determined through the methods above. Then, the separation of quasi-fog zones from land surface and cloud zones is achieved, together with the analysis of probability density histograms of the reflectivity. Afterwards, the information of quasi-fog zones is obtained from remote sensing images.

3.2.2 Fast connective region encoding method based on image run-length encoding

On the basis of the quasi-fog areas determined from meteorological satellites and in accordance with the characteristics of continuous or uninterrupted spatial distributions of fog areas, connected regions are identified, and each region is analyzed and processed as an independent object. For the algorithm to analyze connected regions, encoding is the key to the timeliness and complexity of the required calculation. The aim of encoding the connected regions is to locate all the target objects in the images and to encode all the pixels that belong to the same target object with only one identical mark. By studying the characteristics of all pixels within a whole target object, we obtain the overall performance and parameters of the target being studied. Fig.3 presents a diagram showing the connected regions.

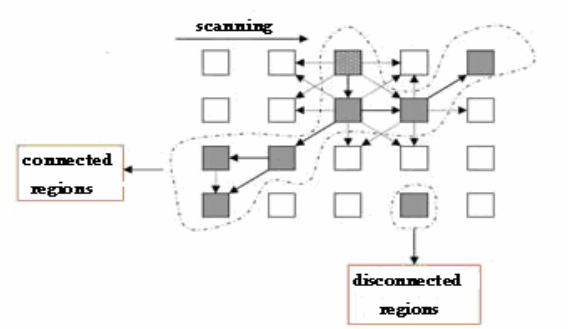

Fig.3 Diagram for connected regions.

To meet the need for a rapid response in fog recognition operations, this paper uses the method of rapid encoding of connected regions based on image run-length codes; that is, a tree is used to describe the relationship between individual run-lengths. By scanning the run-length-described images twice, the connected regions are then encoded rapidly and the transmission of marks within the tree is completed.

This approach is based on the following main technical idea: where the tree has root, trunk, and branches, the corresponding run-length code (RLC) has a root RLC, grandfather RLC, and father RLC. An RLC has a father node RLC, which refers to the existence of RLCs with a neighboring relation node on its upper triangle domain; for example, if the RLC has no parent node RLC, but has a grandfather RLC, then their relative RLC relationship can be established by the father-son relationship in the middle process. A root RLC is an independent RLC (i.e., has neither a father RLC nor a grandfather RLC). All the RLCs belonging to one target have only one root RLC. With the exception of root RLCs, whether an affinity backtracking relationship exists between all the other RLCs and the root RLC, that is, whether any two RLCs belong to one target, can be determined by judging whether the two RLCs have close relationships (or have the same root RLC).

The encoding process involves the analysis of the connectivity of images being run-length encoded. In this article, we use run-length eight-connection for the analysis. The encoding process can be completed by two scans of the run-length encoded images.

The above RLC-based encoding method for

connected regions has the advantages of rapid calculation speed, small storage capacity, and easy realization, thus greatly meeting the need for an operational application to fog detection.

3.2.3 IDENTIFICATION METHOD FOR FOG STRUCTURE CHARACTERISTICS

(1) Analysis of texture fractals

Texture information is the spatial information about images that can perfectly integrate macroscopic properties with structural details. In the mathematic analysis of fractal characteristics, the proposed fractal dimension effectively reflects the textural complexity and roughness and sheds light on its inner self-similarity. In meteorological remote sensing images, clouds differ from fog in the surface texture of grayness; that is, they correspond to different fractal dimensions and have distinct fractal characteristics. While the cloud texture is rough and disorganized, corresponding to large fractal dimensions, the fog texture is fine, corresponding to small fractal dimensions. The fractal dimension can be used to distinguish between clouds and fog. There are many kinds of fractal dimension; for the sake of convenient calculation, we use the method of box fractal dimension analysis to test and analyze the fog. The principles of calculation are as follows:

F is any non-empty subset community in R^n, and $N_d(F)$ is the smallest number of subsets that have the largest diameter of d and can cover F. The set-top box dimension can then be defined as

$$\underline{\mathrm{Dim}}_B F = \lim_{d\to 0} \frac{\log N_d(F)}{-\log d} \tag{5}$$

$$\overline{Dim}_B F = \overline{\lim_{d\to 0}} \frac{\log N_d(F)}{-\log d} \tag{6}$$

If the two values are equal, they can be called the box dimension of F, which is denoted as

$$\mathrm{Dim}_B F = \lim_{d\to 0} \frac{\log N_d(F)}{-\log d} \tag{7}$$

Considering the characteristics of clouds and fog, we chose the method jointly put forward by Sarkar and Chaudhuri and follow the steps below:

① First, the image size is set as $M\times M$ and shrunken according to the scale of s×s, where $1 < s < M/2$ and scale $r = M/s$;

② Then, the image is treated as a three-dimensional space (x, y, z), where (x, y) represents the two-dimensional coordinates and z the image's grayness level; (x, y) is divided into δ×δ areas, and boxes are piled in each of the areas whose bottom area is $\delta\times\delta$ and height is h, where $h = G/r$ and G is the largest grayness level of the image;

③ And next, statistics are done of the number of boxes that pass through the image, N_r. As to the different scale, r, a corresponding number of boxes, N_r, is obtained, with $\log(1/r)$ and $\log(N_r)$ taken as the abscissa and longitudinal respectively. A straight line is drawn, fitting to the corresponding points of $\log(N_r)$ and $\log(1/r)$ by the lease square method.

The slope, K, of the straight line corresponds to the fractal dimension of the image (Fig.4).

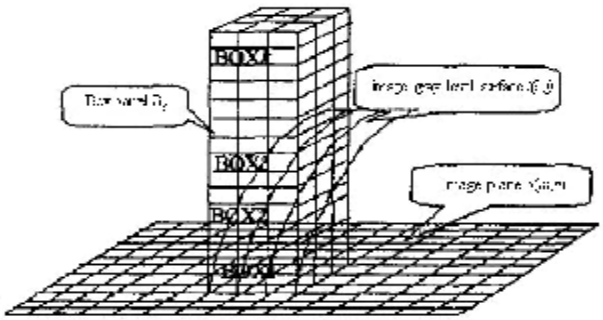

Fig.4 Sketch map for box dimension.

(2) Analysis of shape fractals

As fog zones (excluding those over canyons) have clear and regular boundaries in the visible light band, non-fog zones and other noise areas can be excluded through the analysis of patterns of fog zone boundaries.

The fractal dimension (FD) formula for determining the FD of shape is as follows:

$$\mathrm{FD} = 2\ln(P/4)/\ln(A) \tag{8}$$

where P is the perimeter of a connected region and A is its area. As demonstrated in the experimental calculation, when FD is larger than 1.1, the region can be regarded as a non-fog area, that is, a noise region.

(3) Analysis of smoothness

The analysis of smoothness is a measurement of the fluctuation range of satellite values. In view of the even distribution of fog zones, grayness fluctuates mildly. By adopting the smoothness test, we can detect fog based on the data from the visible light band. If the connected region is unsmooth, it will be less likely to be judged a fog zone.

The formula for smoothness, P, is as follows:

$$P = 1 - \frac{\frac{1}{n}\times\sum_{i=1}^{n}(x_i - \bar{x})^2}{\bar{x}^2} \tag{9}$$

$$\bar{x} = \frac{1}{n}\times\sum_{i=1}^{n} x_i \tag{10}$$

where x_i is the pixel value and n is the number of pixels.

(4) Analysis of template characteristics

While the fog area is characterized by smooth tops, low brightness, and regular and stable spatial distribution, the cloud zone typically has high brightness, unstable spatial distribution, significant fluctuation, and so forth. Satisfactory results can be obtained in cloud/fog recognition and separation using the analysis of template characteristics. The main idea behind the analysis is the adoption of appropriate dimensional templates and the identification of the differences between cloud and fog in distribution patterns and physical characteristics by calculating and analyzing the mean grayness level or physical quantities and variances for consecutive areas. This leads to the automatic separation of fog from clouds.

① Analysis of mean variance

In view of the contrast that fog is uniformly, smoothly, and continuously distributed whereas clouds fluctuate greatly in their spatial distribution and are disorganized in structure, an $n \times n$ dimension template is used to calculate the mean value and mean variance within the template. If the mean value and mean variance simultaneously satisfy the following conditions, then the area can be judged to be fog.

The conditions of $\mu \in [\beta_1, \beta_2]$ and $R^2 < \varepsilon$ are satisfied when the mean value μ and mean variance R^2 are calculated from the respective formula as follows:

$$m = \frac{1}{n}\sum_{i=1}^{n} A_i \quad (i=1,2,3\ldots n) \tag{11}$$

$$R^2 = \frac{1}{n}\sum_{i=1}^{n}\sum_{i=1}^{n}(A_i - m) \quad (i=1,2,3\ldots n) \tag{12}$$

where A_i is the grayness level or physical quantity of the pixel, β_1 and β_2 are the highest and lowest limits of the grayness level or physical quantity of fog that can be known by spectral analysis, and ε is the permissible error of the fog area, which can be obtained experimentally from different meteorological satellite data.

② Analysis of selective averaging method

The $n \times n$ dimension templates are adopted to calculate the mean value, μ, and standard deviation, η, for all the points surrounding the central point (point P) within the template area. If both μ and η for an area can satisfy the following condition, the area is identified as fog.

That is:

$$\mu, P \in [\beta_1, \beta_2]$$
$$\eta < \varepsilon$$

where the mean value, μ, and the standard deviation, η, respectively, are

$$m = \frac{1}{n*(n-1)}\sum_{i=1}^{n} A_i \quad (i=1,2,3\ldots n) \tag{13}$$

$$h = \frac{1}{n*(n-1)}\sum_{i=1}^{n}(A_i - m)^2 \quad (i=1,2,3\ldots n) \tag{14}$$

The meanings of A_i, β_1, β_2, and ε are specified above.

3.2.4 INFRARED BRIGHTNESS TEMPERATURE RECOGNITION METHOD FOR FOG

At night, the satellite only has infrared band data and cannot obtain visible light images; therefore, it is difficult to carry out the cloud/fog identification. As for the characteristics of satellite radiation, since the radiation characteristics of low clouds at night are similar to those of the black body in the thermal infrared channel (about 11 μm), its emissivity is close to 1, while the emissivity of the mid-infrared channel (about 3.7 μm) is significantly less than 1. These differences in emissivity between the two infrared bands of clouds and fog will lead to different brightness temperatures in corresponding infrared cloud images. However, the actual land and oceans do not show such differences. As a result, with coexisting mid-infrared and thermal infrared data, the difference in brightness temperature between the two infrared channels can be used to distinguish between low clouds and fog, following what is also known as the double spectrum method.

3.3 *Comparison of fog detecting methods*

Fog detection can be performed using the method of either spectral analysis or structural analysis. The spectral analysis used in this paper is mainly conducted by isolating the spectral relationship and distribution patterns between fog areas, cloud areas, and land surface from remote sensing images at different time phases, setting the dynamic thresholds to automatically separate fog areas from high clouds, cold clouds, and land surface. Although this method is characterized by strong objectivity, rapid calculating speed, and easy operation, sometimes the same object is captured with a different spectrum. As low clouds, stratus clouds, and fog areas share similar spectra, using the spectral method alone cannot separate the fog area from the cloud area. Further structural analysis is needed to discriminate between them.

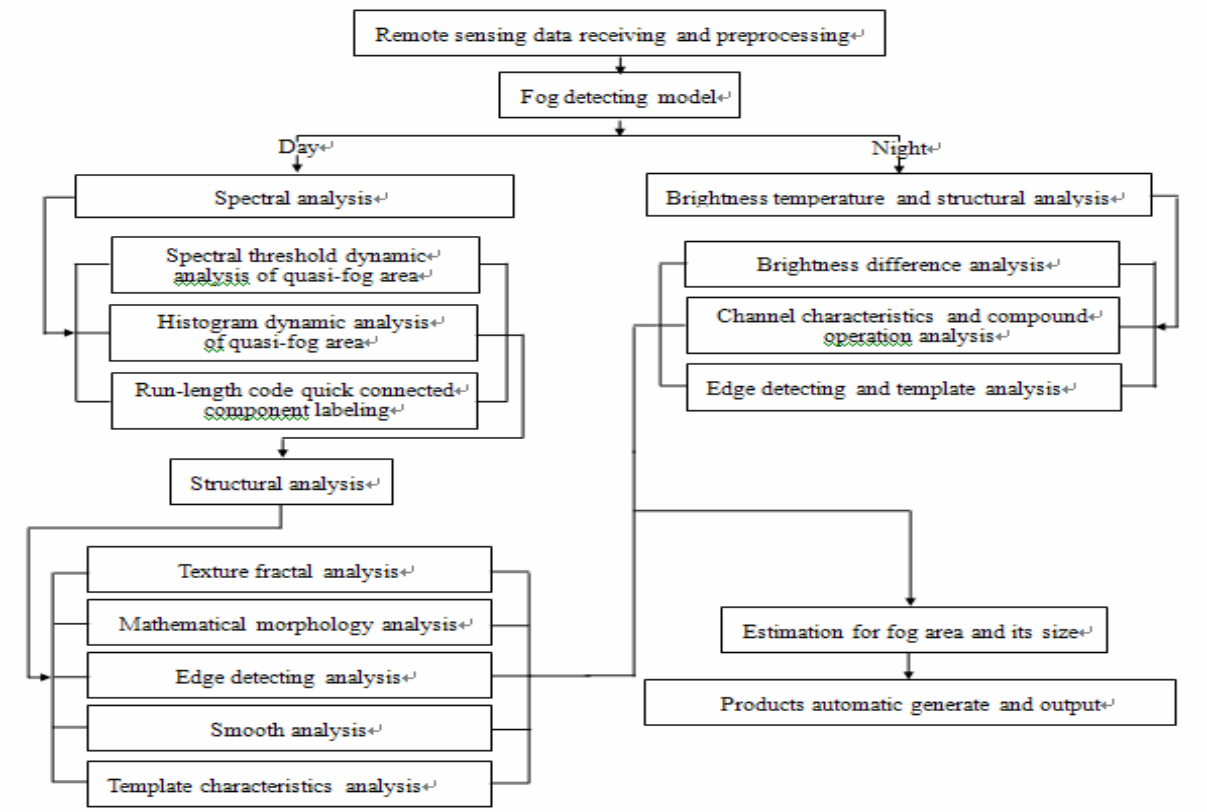

Fig.5 Fog detecting operation process by satellite remote sensing.

Structural analysis works to raise the accuracy of fog detection mainly by studying the conditions of different textures, shapes, smoothness, and edges of the fog area in order to separate fog from clouds. Textural analysis is conducted for cloud/fog isolation and separation according to the fractal dimension (or size of the texture) on the surface of the fog and cloud. It is particularly effective for convective clouds with inconsistent grayness and roughness, and frontal cloud systems, but is less effective in the detection of clouds with smooth tops. Shape analysis is performed to distinguish the cloud area and fog area by analysis of the patterns of the edges of the connected regions. As the edge of the fog area is usually regular, the method will be somewhat effective, but can be misleading when some clouds also have well-defined boundaries. The analysis of smoothness and template characteristics works based on the difference between the fog area with smooth, mildly bright, and regularly distributed tops and the cloud area with large brightness and unstable and varying spatial distribution. Although this method is suitable for detecting convective and frontal clouds, it is somewhat limited in its ability to detect smoothly topped stratus clouds. In this study, we use the separation method of brightness temperature for stratus with similar spectral and textural characteristics because stratus clouds have a lower brightness temperature compared with fog areas.

In summary, each method for the detection of fog has its own advantages and disadvantages. As cloud and fog have similar spectra, and complicated situations like adhesion occur often, separating the complete area of fog from the land surface and cloud zones only by individual characteristics is difficult. Following the principle of cloud/fog detection with remote sensing images and adopting the various practical determining methods presented above, this study identifies and extracts the fog zone using a step-by-step approach to make use of individual advantages and to come to detailed conclusions in a gradual and progressive way.

3.3 *Process of fog detection and cloud / fog separation*

The extraction of information is a prerequisite for the operational application of a fog detection method. The concrete steps of this process are shown below (Fig.5), following the orderly workflow of observing the spectral evidence first and the structural evidence second.

4 ANALYSIS OF APPLICATIONS OF FOG DETECTION

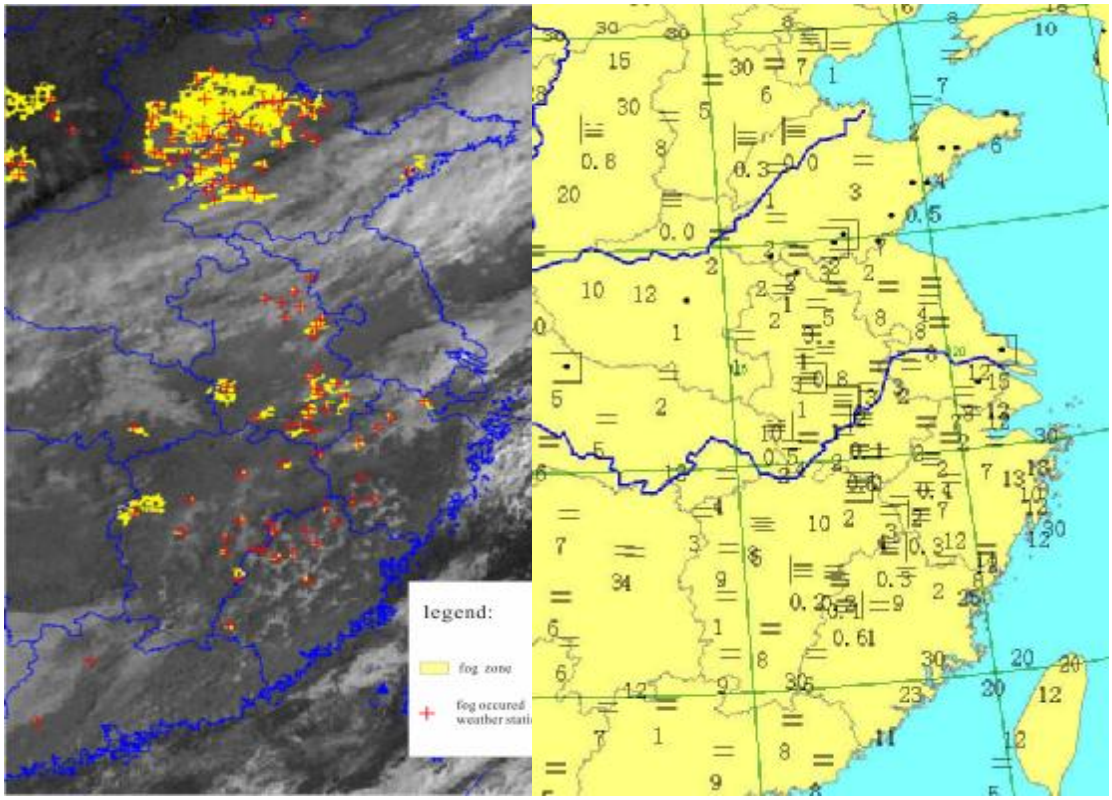

Fig.6 Fog distribution at 00:01 UTC from FY-2C (left panel) and live record at 00:00 UTC (right panel) on Nov.15, 2008.

4.1 *Accuracy of fog detection*

In view of the fact that fog is generated in patches while the observation stations are distributed in points, a point-to-point statistical method is adopted here to analyze the accuracy of the detected fog. The FY-2C remote sensing data is extracted for information about fog areas from 73 frames of images of Shanghai and areas in eastern China in different time phases in recent years (between October 2007 and December 2008) and used as samples to be verified. Simultaneous observations of land surface fog are taken as standards to be checked against. Then, the average relative error is calculated between the fog area from remote sensing and the corresponding one observed over the land surface. If an area is identified with fog by both means, the conclusion is thought to be correct; if it is not, it is considered false. The formula for verification is as follows:

$$\overline{\Delta} = \frac{1}{n}\sum_{i=1}^{n} |W_i - V_i| / V_i \qquad (15)$$

where the $\overline{\Delta}$ is the relative error of the fog area detected by remote sensing, W_i the number of fog points by remote sensing in satellite versus land observation, V_i the number of fog points observed on land surface, and N the number of sample frames of remote sensing images.

According to the verification by the above method, the relative error of fog areas is 21.43% on average.

4.2 *Real cases in application*

4.2.1 CASE 1

Fig.6 shows the fog product that was discriminated and automatically created from the data received by the FY 2C geostationary satellite at 0:01 UTC November 15, 2008 (left panel). It is noted in the figure that a large area of fog occurred at the border between the southeast of Hebei and Shandong provinces and heavy fog occurred in the middle of Shanxi, south of Anhui, Jiangxi provinces. From the calculation, the fog is shown to distribute over an area up to 59,728 km^2. Generally consistent distribution is found from the comparison of the isolated fog zone and the meteorological observations by MICAPS at consecutive times (right panel).

4.2.2 CASE 2

Fig.7 presents the fog product that was discriminated and automatically created by the data received from the NOAA_17 polar-orbiting satellite at 02:13 UTC January 9, 2008 (left panel). As shown in the figure, a heavy fog occurred in the Shanghai area and Jiangsu province, and it was heavy south of Shandong, north of Anhui and north of Zhejiang provinces over an area up to 57,142 km^2. Generally

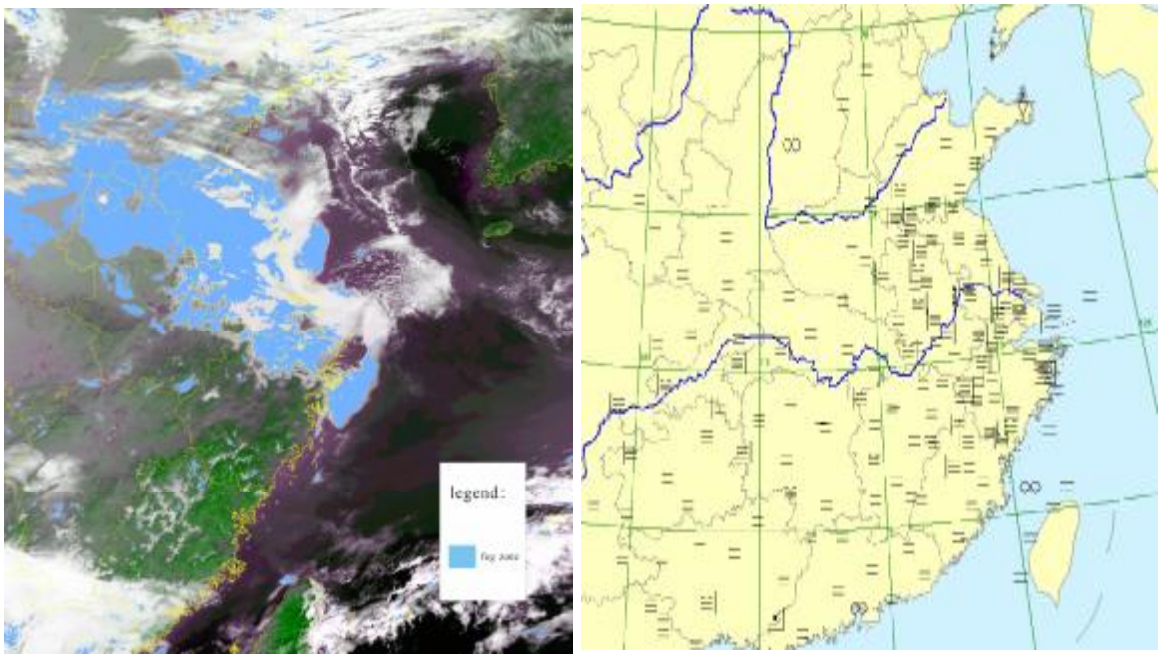

Fig.7 Fog distribution at 02:13 UTC (left panel) and live records at 00:00 UTC (right panel) on Jan. 9, 2007.

consistent distribution is found from the comparison of the isolated fog zone and the meteorological observations by MICAPS at consecutive times (right panel).

5 CONCLUSIONS

(1) According to the different spectral characteristics of land surface media, clouds, and fog zones, relationships are established between the land surface reflectivity and cloud/fog reflectivity of the FY-2C satellite visible light images in different time phases. Dynamic thresholds for determining quasi-fog zones are created automatically by calculating and analyzing the relative change rates of image reflectivity. This method proves effective for the automatic detection of fog and the improvement of the timeliness and objectivity of fog detection.

(2) The rapid, objective, and highly automated remote sensing detection of fog is made possible by a rapid encoding method for connected regions based on image RLCs combined with the analysis of texture and shape fractal patterns, smoothness, template characteristics, and other practical analytic skills.

(3) It is difficult to identify nighttime cloud/fog by remote sensing, as the satellite has the infrared band data only at night and cannot obtain the visible light images. Generally, the differences in brightness temperature between the thermal infrared channel (about 11 μm) and the mid-infrared channel (3.7 μm) are used to distinguish between low-lying clouds and fog. Though effective under some circumstances, this method still falls short in terms of accuracy of recognition.

(4) The above detecting methods for the remote sensing of fog are suitable for both geostationary and polar-orbiting satellites. Under favorable conditions, the accuracy of fog detection will be greatly improved by adopting an approach that combines surface observations (satellite data) and point observations (real-time land surface meteorological data).

REFERENCES:

[1] GURKA J J, OLIVER V J. Fog persistence under a cirrus band [J]. Mon. Wea. Rev., 1974, 102: 869-870.
[2] GUSTAFSON A V, WASSERMAN S E. Use of satellite information in observing and forecasting fog dissipation and cloud formation [J]. Mon. Wea. Rev., 1976, 104: 323-324.
[3] GURKA J J. The role of inward mixing in the dissipation of fog and stratus [J]. Mon. Wea. Rev., 1978, 106: 1633-1635.
[4] EYRE J R, BROWNSCOMBE J L, ALLAM R J. Detection of fog at night using Advanced Very High Resolution Radiometer (AVHRR) imagery [J]. Meteor. Mag., 1984, 113: 266-271.
[5] TURNER J, ALLAM R J, MAINE D R. A case study of the detection of fog at night using channels 3 and 4 on the Advanced Very High Resolution Radiometer (AVHRR) [J]. Meteor. Mag., 1986, 115: 285-297.
[6] KUDOH J, NOGUCHI S. Identification of fog with NOAA AVHRR images [J]. Geosci. Remote Sens., IEEE Transactions on Geoscience and Remote Sensing, 1991: 704-709.
[7] BENDIX J. Determination of fog horizontal visibility by means of NOAA-AVHRR [C]// IEEE 1995 International Geoscience and Remote Sensing Symposium (IGARSS'95),

Piscataway, 1995, 3: 1847-1849.
[8] ELLROD G P. Advances in the detection and analysis of fog at night using GOES multispectral infrared imagery [J]. Wea. Forec., 1995, 10: 606-619.
[9] THOMAS F L, TURK F J, RICHARDSON K. Stratus and fog products using GOES-8-9 3.9μm data [J]. Wea. Forec., 1997, 12: 664-677.
[10] BENDIX J, BERTHMANN F, REUDENBACH C. NOAA-AVHRR and 4D GIS - towards a more realistic view of fog clearance [C]// IEEE 1999 International Geoscience and Remote Sensing Symposium (IGARSS'99), Hamburg, 1999: 2235-2237.
[11] ERASMUS D A. The application of Satellite and Global Meteorological Model data to Monitoring and Forecasting of Moisture and Cloud at Remote Sites in Northern Chile [C]// Sixth International Conference on Southern Hemisphere Meteorology and Oceanography, 1999.
[12] BENDIX J, BERTHMANN F, REUDENBACH C. NOAA-AVHRR and 4D GIS-towards a more realistic view of fog clearance [C]. Geoscience Remote Sensing Symposium, IGARSS '99 Proceedings. IEEE 1999 International, 1999, 4: 2235-2237.
[13] ROSENFELD D, CATTANI Elsa, MELANI S, LEVIZZANI V. Considerations on daylight operation of 1.6-versus 3.7-μm channel on NOAA and Metop satellites [J]. Bull. Am. Meteor. Soc., 2004, 85(6): 873-881.
[14] UNDERWOOD S J, ELLROD G P, KUHNERT A L. A multiple-case analysis of nocturnal radiation-fog development in the central valley of California utilizing the goes nighttime fog product [J]. Appl. Meteor., 2004, 43(2): 297-311.
[15] BACHMANN M, BENDIX J. Fog studies in the Alpine region with NOAA/AVHRR [C]. Geoscience and Remote Sensing Symposium, 1991. IGARSS '91'Remote Sensing: Global Monitoring for Earth Management, 1991: 1713-1716.
[16] BENDIX J, THIES B, NAUSS T, et al. A feasibility study of daytime fog and low stratus detection with TERRA/AQUA-MODIS over land [J]. Meteor. Appl., 2006, 13(2): 111-125.
[17] LIU Jian, XU Jian-ming, FANG Zong-yi. Analyse the scale characteristics of particle on the top of could and fog by the use of AVHRR data of NOAA [J]. J. Appl. Meteor. Sci., 1999, 10(1): 28-33.
[18] JU Wei-min, SUN Han, ZHANG Zhong-yi. The primary applictaion of remote sensing data in heavy fog monitoring of Shanghai-Nanjing high way [J]. Remote Sens. Info., 1997, (3): 25.
[19] LI Ya-chun, SUN Han. Research of remote sensing monitoring of day-time fog by using the data of GMS-5 meteorological satellite [J]. J. Nanjing Inst. Meteor., 2001, 24(3): 343.
[20] LI Ya-chun, SUN Han, XU Meng. The existing problem in the application of meteorological remote sensing fog monitoring [J]. J. Appl. Meteor. Sci., 2000, 15(4): 223-227.
[21] ZHOU Hong-mei, TAN Jian-guo, GE Wei-qiang, YANG Chong-jun. NOAA Satallite Could and Fog Automatic Detecting and Reparation Method [J]. J. Nat. Disaster, 2003, 12(3): 41-47.

Citation: ZHOU Hong-mei, GE Wei-qiang and BAI Hua et al. Research on automatic fog identification technology by meteorological satellite remote sensing. *J. Trop. Meteor.*, 2009, 15(1): 28-37.